

DOI <https://doi.org/10.1007/s11595-018-1885-x>

Synthesis and Characterization of Rectorite/ZnO/TiO₂ Composites and Their Properties of Adsorption and Photocatalysis for the Removal of Methylene Blue Dye

WANG Huanhuan¹, ZHOU Peijiang^{1*}, WANG Jia¹, WANG Yifei¹, WEI Junchong², ZHAN Hongju³, GUO Rui¹, ZHANG Yali¹

(1. School of Resource and Environmental Science, Hubei Biomass-Resource Chemistry and Environmental Biotechnology Key Laboratory, Eco-environment Technology R&D and Service Center, Wuhan University, Wuhan 430079, China; 2. School of Materials Science and Engineering, Wuhan University of Technology; 3. Jingchu University of Technology, Jingmen 448000, China)

Abstract: As efficient water treatment agents, a novel series of rectorite-based ZnO and TiO₂ hybrid composites (REC/ZnO/TiO₂) were synthesized and characterized in this study. Effects of experimental parameters including TiO₂ mass ratio, solution pH and catalyst dosage on the removal of methyl blue (MB) were also conducted. The presence of a little mass ratio (2%-6%) of TiO₂ highly promoted the photoactivity of REC/ZnO/TiO₂ in removal of MB dye from aqueous solution, in which ZnO and REC played a role of photocatalyst and adsorbent. The promotion effects of TiO₂ may result from the accelerated separation of electron-hole on ZnO. The observed kinetic constant for the degradation of MB over REC/ZnO and REC/ZnO/TiO₂ were 0.015 and 0.038 min⁻¹, respectively. The degradation kinetics of MB dye, which followed the Langmuir-Hinshelwood model, had a reaction constant of 0.17 mg/(L · min). The decrease of removal ratio of MB after five repetitive experiments was small, indicating REC/ZnO/TiO₂ has great potential as an effective and stable catalyst.

Key words: TiO₂; ZnO; methylene blue; photocatalysis; rectorite

1 Introduction

Parallel with population growth and society development, over 7×10^5 tons per year of organic dyes in estimated are widely used in various industries^[1]. According to statistics, approximately 2% of these organic dyes would finally be introduced into the discharged effluents, which causes a number of serious environmental problems for water pollution due to the severe color and the high oxygen demand^[2,3]. Therefore, dye wastewater is one of the earnest environmental issues

in urgent need to be solved in the environmental remediation realm.

Photocatalysis which utilizes renewable solar energy to activate the chemical reactions via oxidation and reduction could be an effective wastewater treatment technology^[4,5]. This photocatalysis system has attracted great interest from science community as the most promising way to solve the environmental problems, especially getting rid of residual dyes pollutants from wastewater stream because of its potential high activity, low energy consumption, mild treatment conditions, and ease of handling^[6-11]. The irradiation of semiconductors by UV-visible light produces hydroxyl radicals ($\bullet\text{OH}$) and singlet oxygen ($^1\text{O}_2$), and these reactive oxygen species (ROS) can efficiently oxidize or mineralize organic compounds. Moreover, direct reaction between valence-band holes and organic compounds can also induce oxidation or decomposition of target organic pollutants. The contributions of ROS and holes toward the degradation of organic pollutants depend on the electronic properties of the target substance and the photocatalyst^[12,13].

Many semiconducting materials such as zinc oxide (ZnO), titanium dioxide (TiO₂), cuprous oxide (Cu₂O) are used for the removal of organic dyes from

© Wuhan University of Technology and Springer-Verlag GmbH Germany, Part of Springer Nature 2018

(Received: Dec. 11, 2016; Accepted: Mar. 16, 2018)

WANG Huanhuan(王欢欢): Ph D; E-mail: doublewhh@163.com

* Corresponding authors: ZHOU Peijiang(周培疆): Prof.; Ph D; E-mail: zhoupj@whu.edu.cn

Funded by the National High Technology Research and Development Program of China (No. 2007AA06Z418), the National Natural Science Foundation of China (Nos. 20577036, 20777058, 20977070), the National Natural Science Foundation of Hubei Province, China (No.2015CFA137), the Open Fund of Hubei Biomass-Resource Chemistry and Environmental Biotechnology Key Laboratory (Wuhan University), and the Fund of Eco-environment Technology R&D and Service Center (Wuhan University)

the wastewater due to their unique properties in photocatalysis^[14-17]. Among many semiconductors, ZnO and TiO₂ are the most widely studied photocatalysts because of their high catalytic activity, resistance to chemical and optical corrosion, and non-toxic and stable chemical properties^[18-21]. However, high electron-hole recombination rate make ZnO or TiO₂ not a high efficient catalyst. Many strategies such as ion doping, modified with photo-sensitizer, semiconductor compositions have been applied to improve the photocatalysis efficiency. Recently, it has been reported that ZnO and TiO₂ composites possessed higher photocatalytic activity than either ZnO or TiO₂^[22-25].

To improve the performance of photocatalyst, another strategy has focused on the development of composites based on clay minerals that enhance the photocatalytic efficiency via improved adsorption^[26-32]. As a kind of silicate clay mineral, rectorite (REC) is composed of alternating pairs of nonexpendable dioctahedral mica-like and expandable dioctahedral smectite-like layers^[33], which can efficiently adsorb organic compounds both on its external surfaces and within its interlaminar spaces due to its high specific surface area and ion exchange properties^[34]. Because of its low cost, small size, and unusual intercalated structure, REC also arouses great interest as a catalyst support. Considerable researches have been devoted to exploring the application of REC-based composite materials to adsorb or catalytically decompose environmental pollutants^[35-37].

In this study, a novel REC/ZnO/TiO₂ composite was prepared by an improved hydrothermal process. The composite was characterized by scanning electron microscopy (SEM), transmission electron microscopy (TEM), and X-ray powder diffraction (XRD). The absorption and photocatalytic performance of REC/ZnO/TiO₂ were systematically evaluated by the removal of methylene blue (MB) dye under simulated sunlight irradiation. The degradation intermediates were also identified by liquid chromatography-mass spectrometry (LC-MS).

2 Experimental

2.1 Chemicals

Methylene blue (MB), ethylene glycol, hydrazine hydrate, dimethyl benzene, ethyl alcohol, zinc acetate dihydrate (Zn(CH₃COO)₂•2H₂O) (purity: 99.9%) and sodium hydroxide were of analytical grade, and they were provided by Alpha-Aesar and used as-received.

P25 titanium dioxide was purchased from Degussa, Germany. Refined REC was purchased from Hubei Mingliu Inc. Co. (Wuhan, China). The water used in the experiments had been pretreated by an ultrapure water system (Liyuan Electric Instrument Co., Beijing, PRC).

2.2 Synthesis of REC/ZnO/TiO₂

The REC/ZnO/TiO₂ composite was prepared via a hydrothermal process. Specifically, 2.1951 g (10 mmol) of Zn(CH₃COO)₂•2H₂O were dissolved in 200 mL of a mixed solvent of dimethyl benzene and ethylene glycol at 300 rpm for 30 min. Then, a solution of hydrazine hydrate (0.726 mL, 15 mmol) in anhydrous ethanol (30 mL) was added dropwise to the suspension and stirred for another 1 h. Then, the appropriate calculated weights of REC and TiO₂ (weight ratios of REC/ZnO/TiO₂ were 2:1:0.057, 2:1:0.067, 2:1:0.08, 2:1:0.1, and 2:1:0.2.) was added to this ZnO colloid solution. The resulting dispersion was vigorously stirred for 5 h at room temperature. Centrifugation provided the REC/ZnO/TiO₂ composites as gray solids. These solids were rinsed three times with anhydrous ethanol and another three times with deionized water, and calcined for 5 h in a muffle furnace at 500 °C.

2.3 Characterization of the synthesized materials

The Brunauer-Emmett-Teller (BET) surface area was determined using a Micromeritics model ASAP 2020 (Norcross, GA) instrument. The XRD patterns of the products were determined using a Dmax-rA powder diffractometer (Rigaku, Japan), which used Cu K α radiation source at a scanning rate of 2° min⁻¹. SEM images and energy-dispersive X-ray spectroscopy (EDS) data were acquired using a QUANTA 200 (FEI, USA) instrument. Transmission electron microscopy (TEM) images were obtained with a JEM 2010HT instrument (JEOL, Japan) at an accelerating voltage of 200 kV.

2.4 Photocatalytic degradation of MB dye under simulated solar radiation

Photodegradation of MB dye was carried out in a YM-GHX-V II photoreactor (Shanghai Yumin Instruments Ltd., Shanghai, China). Aqueous solutions of MB dye (200 mL; initial concentration: 5 to 25 mg/L) were mixed magnetically with the various catalysts in a 250 mL Pyrex beaker. After equilibrating in the dark for 1 h, aliquots (2 mL) of those suspensions were withdrawn to determine the initial MB concentration, c_0 . Aliquots (2 mL) were also collected at selected time intervals as the MB degraded; these were magnetically separated and used to determine c_t . The degradation of the MB

dye was monitored using a 2550 UV-visible spectrophotometer (Shimadzu, Japan) with a 10-mm cuvette. The slope of a linear fit of the data provided the initial photodegradation rate, R_0 (mg/Lmin).

2.5 Sample and data analyses

Sample analysis: The MB dye concentration was determined according to its absorbance at 665 nm.

Data analysis: The removal ratio (R , %) of the MB dye was calculated using Eq.(1):

$$R = (1 - \frac{c_t}{c_0}) \times 100\% \quad (1)$$

The kinetics of MB degradation (pseudo-first-order rate constant) were determined from the regression of the slope of a plot of MB concentration *versus* time using Eq. (2):

$$c_t = c_0 e^{-k_{obs} \times t} \quad (2)$$

c_t and c_0 represent the concentration of MB at reaction time t and the initial concentration, respectively. k_{obs} (min^{-1}) represents the observed transformation kinetic constants of MB.

3 Results and discussion

3.1 XRD and morphology of REC/ZnO/TiO₂ composites

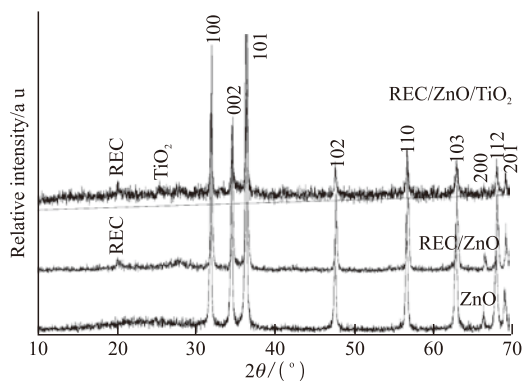


Fig.1 XRD patterns of ZnO, REC/ZnO, and REC/ZnO/TiO₂ (2:1:0.067)

As demonstrated in Fig.1, peaks observed at 31.7, 34.4, 36.2, 47.5, 56.5, 62.8, 66.3, 67.9, and 69.0° were indexed to hexagonal wurtzite (ZnO; JCPDS Data Card no. 36-1451). Additional peaks appeared at ca. 28.2° in REC/ZnO that corresponded to REC^[38]. The peak at $2\theta = 25.4^\circ$ confirms that there is anatase phase in the REC/ZnO/TiO₂ composite^[39], whereas 2θ at 37.8° and 47.7° for anatase TiO₂ and 2θ at 27.5° and 36.1° *etc* for rutile TiO₂ are too weak to be observed because of TiO₂'s small mass ratio (2.2%) in the composite^[40]. XRD re-

sults indicated that the introduction of both ZnO and TiO₂ into REC.

The morphologies of REC/ZnO/TiO₂ were investigated by TEM and SEM and the results were demonstrated in Fig.2. It has been well documented that REC is an interstratified clay mineral^[38]. Small particles appeared in SEM and TEM image of REC/ZnO/TiO₂ besides of interstratified clay mineral, indicating the binding of ZnO and TiO₂ to REC.

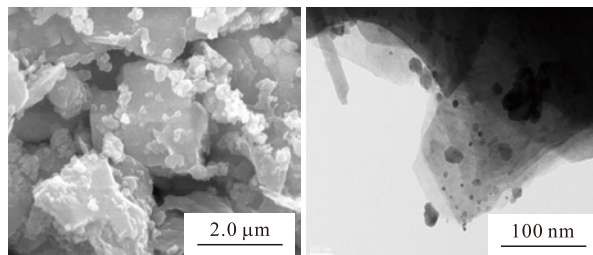


Fig.2 (a) SEM image and (b) TEM image of REC/ZnO/TiO₂ (2:1:0.067)

3.2 Degradation of MB over different catalysts

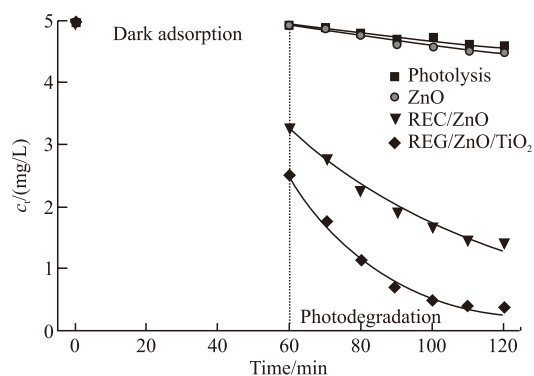


Fig.3 Direct photolysis, and adsorption-photodegradation of MB (5 mg/L) in ZnO, REC/ZnO and REC/ZnO/TiO₂ (2:1:0.067) dispersion (0.7 g/L), pH=6.0 (curves demonstrated the fitting of experimental data with Eq.(2))

Direct photolysis and photodegradation of MB over different catalysts are shown in Fig.3. Only little part of MB was directly decomposed under UV-vis irradiation, indicating MB is photo inert. The adsorption of MB onto ZnO is negligible and ZnO also showed low efficiency in removal of MB under irradiation. Conversely, the adsorption of MB on REC/ZnO was much larger than that on native ZnO. The enhanced adsorption efficiency of MB (36%) was mainly because of the REC, which has been proven to be an efficient adsorbent for MB and other dyes^[41, 42]. The adsorption reached equilibrium within 40 min, and the concentration of MB gradually decreased under irradiation. The degradation ratio reached approximately 70% after 60 min irradiation in 0.7 g/L REC/ZnO dispersion.

The adsorption capacity of REC/ZnO/TiO₂ is larger than that of REC/ZnO. More importantly, REC/ZnO/TiO₂ exhibited higher photoactivity in removal of MB from aqueous solutions. The k_{obs} in REC/ZnO/TiO₂ dispersion (0.038 min⁻¹) is 2.4 times that of REC/ZnO. The enhanced performance of REC/ZnO/TiO₂ composite might result from the facilitated electron-hole separation over ZnO by the presence of TiO₂. Recently, Yang *et al.* have also found that the photocatalytic ozonation degradation of salicylic acid by ZnO modified TiO₂ is much faster than using native TiO₂^[22].

3.3 Effect of component mass ratio on the degradation of MB

The fabricated composites contained REC, ZnO, and TiO₂ and the impact of the component mass ratio on the removal of MB dye was investigated to obtain the optimized composition. Fig.4 shows that the dark adsorption of MB dye on REC/ZnO/TiO₂ was only slightly influenced by the TiO₂ content. After a 60-min adsorption period, the MB dye concentration in the bulk phase decreased by approximately 40% and 50% with TiO₂ contents of 0.057 and 0.067, respectively. The k_{obs} also increased from 0.030 to 0.037 min⁻¹ with the increase of TiO₂ content from 0.057 to 0.067. However, both dark adsorption and photodegradation of MB dye decreased with further increase of TiO₂ content to 0.2.

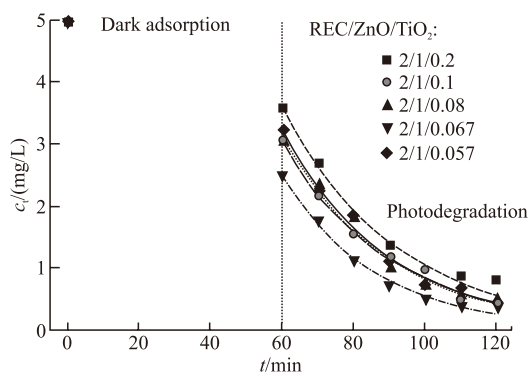


Fig.4 Effects of TiO₂ mass contents of REC/ZnO/TiO₂ (0.7 g/L) on the adsorption and photodegradation of MB dye (5 mg/L), pH=6.0

The enhanced performance of REC/ZnO/TiO₂ may result from the fast electron-hole separation in the presence of TiO₂, and this process could be strengthened with the increase of TiO₂ content. However, TiO₂ also has high absorption in particular in UV region that could compete for irradiation photon with ZnO, and therefore, the photoactivity of REC/ZnO/TiO₂ decreased with continuous increase of TiO₂ in the composites. Similar results have been reported for different

ZnO based composites^[43,44]. For example, the optimized In₂O₃ dosage for hydrogen production under visible light by using In₂O₃/ZnO composites is 10%, further increase of In₂O₃ ratio also decreased the activity of In₂O₃/ZnO^[43].

3.4 Effect of REC/ZnO/TiO2 dosage on the removal of MB dye

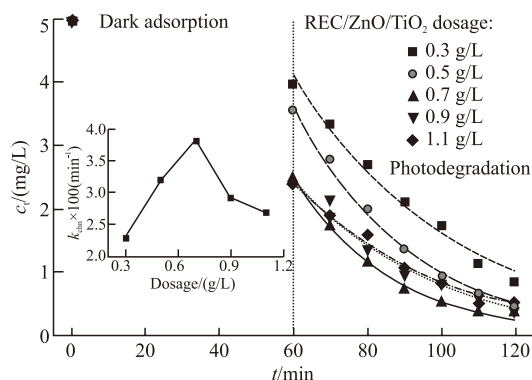


Fig.5 Effect of REC/ZnO/TiO₂ dosage on the adsorption and photodegradation of MB dye (5 mg/L), pH=6.0

The photodegradation of MB aqueous solutions with various REC/ZnO/TiO₂ concentrations was illustrated in Fig.5. Apparently, in this work, the observed photodegradation kinetic constant (k_{obs}) of MB sharply increased when the concentration of REC/ZnO/TiO₂ increased from 0.0 to 0.7 g/L. This result was consistent with many studies where the reaction was accelerated with the increase of catalyst dosage, which was mainly because the amount of reactive species like •OH was determined by the concentration of catalyst in the bulk solution. Conversely, continuously increase of REC/ZnO/TiO₂ decreased the photodegradation of MB, although the dark adsorption was benefited with increase of catalyst. The k_{obs} were 0.038 and 0.027 min⁻¹ in 0.7 and 1.1 g/L REC/ZnO/TiO₂ dispersion. The optimum amount of REC/ZnO/TiO₂ should be added in order to avoid superfluous catalyst and also to ensure total absorption of radiation photons for efficient photodegradation^[45,46]. It could expect an increase of adsorption sites and ROS with increasing of catalyst dosage in a certain region. However, high concentration of REC/ZnO/TiO₂ particles became much easier to aggregate and reduced the light transmission. Therefore, the optimized concentration of REC/ZnO/TiO₂ was fixed at 0.7 g/L.

3.5 Effect of solution pH on the degradation of MB dye

The effect of solution pH was studied in the range of 5.0-9.0 in 0.7 g/L REC/ZnO/TiO₂ dispersion, and the results were demonstrated in Fig.6. The results

indicated that pH value had a significant effect on the activity of REC/ZnO/TiO₂. The favored result for MB degradation was obtained near neutral solution with a maximum at pH 6.0, whereas, removal ratio decreased in the alkaline or acidic pH range.

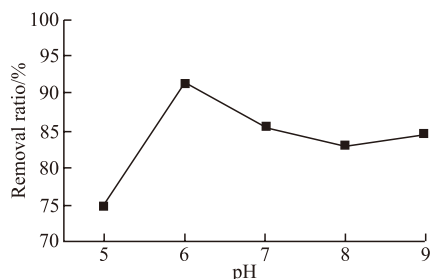


Fig.6 Effect of solution pH on the adsorption and photodegradation of MB dye on REC/ZnO/TiO₂

It was well known that the interpretation of pH effects on the photodegradation of organic pollutants was quite difficult, and the effects of pH on the photocatalytic degradation process were generally related to its multiple roles such as electrostatic interactions between the semiconductor surface, solvent molecules, substrate and charged radicals formed during the reaction process. Hydroxyl radicals are considered as the predominant species at neutral or high pH levels^[45]. Although it was suggested that in alkaline solution •OH are easier to be formed by oxidizing more hydroxide ions available on TiO₂ or ZnO surface^[45,47], it should be noted that in alkaline solution there is a Coulombic repulsion between the negative charged surface of photocatalyst and the hydroxide anions as well as the repulsion between the negative charged surface and the negative form of MB. This fact could decrease the photodegradation of MB at high pH.

3.6 Kinetics for the degradation of MB dye on REC/ZnO/TiO₂

The photodegradation of MB was performed with initial concentrations ranged from 5.0 to 25.0 mg/L. The initial rate (r_0 , mg/L min) for the photodegradation of MB increased with increasing the initial concentration of MB. For example, r_0 increased from 0.063 to 0.15 mg/L•min with its initial concentration from 5 to 25 mg/L. The data were then fitted to the Langmuir–Hinshelwood kinetics rate model Eq. (3), which has been applied to the initial rates of photocatalytic degradation of many organic compounds.

$$r_0 = -\frac{dc}{dt} = k_{re} K_s c_0 / (1 + K_s c_0) \quad (3)$$

where c_0 is the initial concentration of MB after the dark adsorption. k_{re} is the reaction rate constant and K_s represents Langmuir adsorption constant.

The results shown in inset Fig.7 clearly demonstrated the experimental data fit Langmuir–Hinshelwood kinetic model well (correlation factor is 0.99). The recovered k_{re} is 0.17 mg/L min.

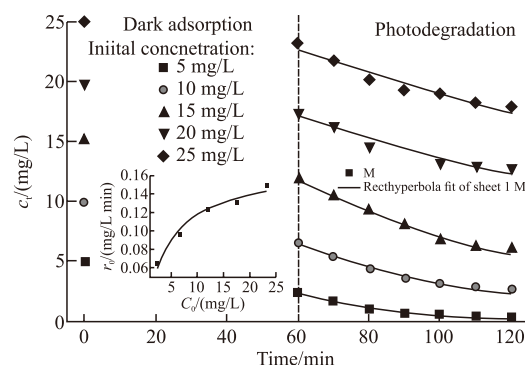


Fig.7 Correlation between the initial rate of loss of MB dye on REC/ZnO/TiO₂ and the initial dye concentration (Inset: The solid line represents fitting of the data to the Langmuir–Hinshelwood kinetic model (Eq.3))

3.7 Reusability of REC/ZnO/TiO₂

Sequential photodegradation experiments were performed to test the photo-stability of catalyst. As shown in Fig.8, the decreasing trend in the final degradation efficiency was approximately 30% after 5 repetitive experiments for REC/ZnO/TiO₂. This result showed that REC/ZnO/TiO₂ possesses potential to be an effective and stable catalyst.

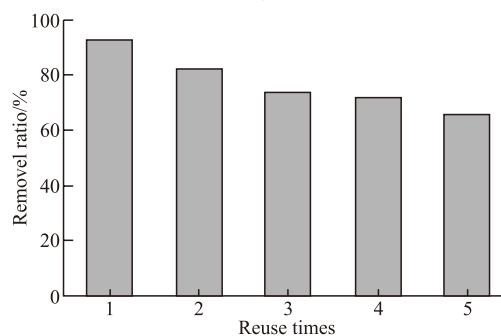


Fig.8 Performance and recovery of 0.7 g/L REC/ZnO/TiO₂ (2:1:0.067) for five cycles

3.8 Mechanism for the degradation of MB dye on REC/ZnO/TiO₂

Intermediates with m/z of 318, 274, and 222 were detected by LC/MS analysis (Fig.9). The intermediate with $m/z = 317$ could be formed through the addition of two •OH radicals per MB dye molecule, or through oxidation of methyl (–CH₃) groups of the sulfoxide intermediate. Addition of •OH to the intermediate of $m/z = 318$ and a loss of a methyl group could produce an intermediate with $m/z = 274$. Oxidation of MB dye could follow different paths. For example, addition of •OH to MB dye molecules would lead to the formation of an intermediate with $m/z = 300$ ^[48]. Oxidation of sul-

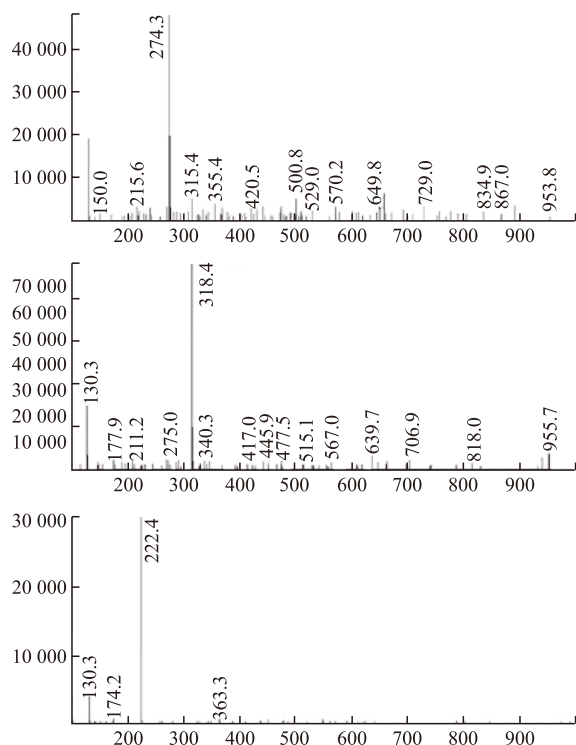


Fig.9 HPLC mass spectrogram of MB photodegradation samples

fur atoms and bond cleavage at nitrogen-bridged sites would lead to the formation of a sulfoxide intermediate having $m/z = 303$ ^[49]. However, neither $m/z = 300$ nor 303 was detected in the present study. Oxidation of these intermediates could form intermediate with small molecular weight or ring cleavage products, and even mineralization to CO_2 and H_2O .

4 Conclusions

A series of REC/ZnO/TiO₂ composites was synthesized and the structure was well characterized. The ZnO component played a major role of photocatalyst and REC played a role of adsorbent. The presence of TiO₂ significantly enhanced the photoactivity of REC/ZnO/TiO₂ in removal of MB from aqueous solutions, with the increase intensity dependent on TiO₂ mass ratio. The optimized pH and dosage for removal of MB is pH 6.0 and 0.7 g/L, respectively. The degradation of MB over REC/ZnO/TiO₂ followed the Langmuir–Hinshelwood model. Repeat usage also demonstrated that REC/ZnO/TiO₂ composite was photo-stable and has great potential as catalysts for the treatment of dye pollutants in aqueous solutions.

References

- [1] Gupta V K, Suhas. Application of Low-Cost Adsorbents for Dye Removal A Review[J]. *J. Environ. Manage.*, 2009, 90(8): 2 313-2 342
- [2] Pearce C I, Lloyd J R, Guthrie J T. The Removal of Colour from Textile Wastewater using Whole Bacterial Cells: A Review[J]. *Dyes. Pigments*, 2003, 58(3): 179-196
- [3] Wang J, Bai R. Formic Acid Enhanced Effective Degradation of Methyl Orange Dye in Aqueous Solutions under UV-Vis Irradiation[J]. *Water Res.*, 2016, 101: 103-113
- [4] Kudo A, Miseki Y. Heterogeneous Photocatalyst Materials For Water Splitting[J]. *Chem. Soc. Rev.*, 2009, 38: 253-278
- [5] Lee K M, Lai C W, Ngai K S, *et al.* Recent Developments of Zinc Oxide Based Photocatalyst in Water Treatment Technology: A Review[J]. *Water Res.*, 2016,88: 428-448
- [6] Zhang X, Wang Y, Liu B, *et al.* Heterostructures Construction on TiO₂ Nanobelts: A Powerful Tool for Building High-Performance Photocatalysts[J]. *Appl. Catal. B-Environ.*, 2017, 202: 620-641
- [7] Tan C, Cao X, Wu XJ, *et al.* Recent Advances in Ultrathin Two-Dimensional Nanomaterials[J]. *Chem. Rev.*, 2017, 117(9): 6 225-6 331
- [8] Pirhashemi M, Habibi-Yangjeh A. Ultrasonic-Assisted Preparation of Plasmonic ZnO/Ag/Ag₂WO₄ Nanocomposites with High Visible-Light Photocatalytic Performance for Degradation of Organic Pollutants[J]. *J. Colloid Interface Sci.*, 2017, 491: 216-229
- [9] Karunakaran C, Dhanalakshmi R. Photocatalytic Performance of Particulate Semiconductors under Natural Sunshine Oxidation of Carboxylic Acids[J]. *Sol. Energ. Mater. Sol. C.*, 2008, 92(5): 588-593
- [10] Madhavan J, Muthuraaman B, Murugesan S, *et al.* Peroxomonosulphate, an Efficient Oxidant for The Photocatalysed Degradation of A Textile Dye, Acid Red 88[J]. *Sol. Energ. Mater. Sol. C.*, 2006, 90(13): 1 875-1 887
- [11] Chen Z, Shuai L, Zheng B, *et al.* Synthesis of Zinc Oxide Nanoparticles with Good Photocatalytic Activities under Stabilization of Bovine Serum Albumin[J]. *J. Wuhan. Univ. Technol.*, 2017, 32(5): 1 061-1 066
- [12] Zhang G, Lan Z A, Wang X. Conjugated Polymers: Catalysts for Photocatalytic Hydrogen Evolution[J]. *Angew. Chem. Int. Ed.*, 2016, 55(51): 15 712-15 727
- [13] Zhang L, Li J, Chen Z, *et al.* Preparation of Fenton Reagent with H₂O₂ Generated by Solar Light-Illuminated Nano-Cu₂O/MWNTs Composites[J]. *Appl. Catal. A-Gen.*, 2006, 299(1): 292-297
- [14] Nagaraju G, Manjunath K, Ravishankar T N, *et al.* Ionic liquid-Assisted Hydrothermal Synthesis of TiO₂ Nanoparticles and Its Application in Photocatalysis[J]. *J. Mater. Sci.*, 2013, 48(24): 8 420-8 426
- [15] Saikia L, Bhuyan D, Saikia M, *et al.* Photocatalytic Performance of ZnO Nanomaterials for Self Sensitized Degradation of Malachite Green Dye under Solar Light[J]. *Appl. Catal. A-Gen.*, 2015, 490: 42-49
- [16] Li G L, Ma P, Zhang Y F, *et al.* Synthesis of Cu₂O Nanowire Mesocrystals using PTCDA as a Modifier and Their Superior Peroxidase-Like Activity[J]. *J. Mater. Sci.*, 2016, 51(8): 3 979-3 988
- [17] Sarkar A K, Saha A, Tarafder A, *et al.* Efficient Removal of Toxic Dyes Via Simultaneous Adsorption and Solar Light Driven Photodegradation using Recyclable Functionalized Amylopectin-TiO₂-Au Nanocomposite[J]. *ACS Sustainable Chem. Eng.*, 2016, 4(3):1 679-1 688
- [18] Fujishima A, Zhang X, Tryk D. TiO₂ Photocatalysis and Related Surface Phenomena[J]. *Surf. Sci. Rep.*, 2008, 63(12): 515-582
- [19] Reddy K R, Karthik K V, Prasad S B B, *et al.* Enhanced Photocatalytic Activity of Nanostructured Titanium Dioxide/Polyaniline Hybrid Photocatalysts[J]. *Polyhedron*, 2016, 120: 169-174
- [20] Podporska-Carroll J, Myles A, Quilty B, *et al.* Antibacterial Properties of F-Doped ZnO Visible Light Photocatalyst[J]. *J. Hazard. Mater.*, 2017, 324: 39-47
- [21] Yi S H, Choi S K, Jang J M, *et al.* Low-Temperature Growth of ZnO Nanorods by Chemical Bath Deposition[J]. *J. Colloid Interface Sci.*,

- 2007, 313(2): 705-710
- [22] Yang T, Peng J, Zheng Y, *et al.* Enhanced Photocatalytic Ozonation Degradation of Organic Pollutants by ZnO Modified TiO₂ Nanocomposites[J]. *Appl. Catal. B-Environ.*, 2017, 221: 223-234
- [23] Ramírez-Ortega D, Meléndez AM, Acevedo-Peña P, *et al.* Semi-conducting Properties of ZnO/TiO₂ Composites by Electrochemical Measurements and Their Relationship with Photocatalytic Activity[J]. *Electrochim. Acta*, 2014, 140(27): 541-549
- [24] Cheng C, Amini A, Zhu C, *et al.* Enhanced Photocatalytic Performance of TiO₂-ZnO Hybrid Nanostructures[J]. *Sci. Rep.*, 2014, 4(8): 4 181
- [25] Sethi D, Sakthivel R. ZnO/TiO₂ Composites for Photocatalytic Inactivation of Escherichia Coli[J]. *J. Photochem. Photobiol. B*, 2017, 168: 117-123
- [26] Jo W K, Clament S S N. Enhanced Visible Light-Driven Photocatalytic Performance of ZnO-g-C₃N₄ Coupled with Graphene Oxide as a Novel Ternary Nanocomposite[J]. *J. Hazard. Mater.*, 2015, 299: 462-470
- [27] Gu N, Gao J, Wang K, *et al.* ZnO-Montmorillonite as Photocatalyst and Flocculant for Inhibition of Cyanobacterial Bloom[J]. *Water Air Soil Poll.*, 2015, 226(5): 1-12
- [28] Kolodziejczak-Radzimska A, Jesionowski T. Zinc Oxide-From Synthesis to Application: A Review[J]. *Materials*, 2014, 7(4): 2 833-2 881
- [29] Feng X, Guo H, Patel K, *et al.* High Performance, Recoverable Fe₃O₄-ZnO Nanoparticles for Enhanced Photocatalytic Degradation of Phenol[J]. *Chem. Eng. J.*, 2014, 244(10): 327-334
- [30] Ökte AN, Karamanis D. A Novel Photoresponsive ZnO-Flyash Nanocomposite for Environmental and Energy Applications[J]. *Appl. Catal. B-Environ.*, 2013, 142-143(10): 538-552
- [31] Ahmad M, Ahmed E, Hong ZL, *et al.* A Facile One-Step Approach to Synthesizing ZnO/Graphene Composites for Enhanced Degradation of Methylene Blue under Visible Light[J]. *Appl. Surf. Sci.*, 2013, 274(1): 273-281
- [32] Wang C, Shi H, Li Y. Preparation of Bentonite Supported Nano Titanium Dioxide Photocatalysts by Electrostatic Self-Assembly Method[J]. *J. Wuhan. Univ. Technol.*, 2012, 27(4):603-607
- [33] Bailey S W, Brindley G W, Kodama H, *et al.* Report of the Clay-Minerals-Society Nomenclature Committee for 1980-1981 Nomenclature for Regular Interstratifications[J]. *Clay. Clay. Miner.*, 1982, 30(1): 76-78
- [34] Guo Y, Zhang G, Gan H. Synthesis, Characterization and Visible Light Photocatalytic Properties of Bi₂WO₆/Rectorite Composites[J]. *J. Colloid Interface Sci.*, 2012, 369(1): 323-329
- [35] Lu Y, Chang P R, Zheng P, *et al.* Rectorite-TiO₂-Fe₃O₄ Composites: Assembly, Characterization, Adsorption and Photodegradation[J]. *Chem. Eng. J.*, 2014, 255(255): 49-54
- [36] Wu S, Fang J, Xu W, *et al.* Bismuth-Modified Rectorite with High Visible Light Photocatalytic Activity[J]. *J. Mol. Catal. A-chem.*, 2013, 373(3): 114-120
- [37] Zhang Y, Guo Y, Zhang G, *et al.* Stable TiO₂/Rectorite: Preparation, Characterization and Photocatalytic Activity[J]. *Appl. Clay. Sci.*, 2011, 51(3): 335-340
- [38] Hanlie H, Xiaoling Z, Miao W, *et al.* Morphological Characteristics of (K, Na)-Rectorite from Zhongxiang Rectorite Deposit, Hubei, Central China[J]. *J. China Univ. Geosci.*, 2008, 19(1): 38-46
- [39] Chen Y, Zhang X, Mao L, *et al.* Dependence of Kinetics and Pathway of Acetaminophen Photocatalytic Degradation on Irradiation Photon Energy and TiO₂ Crystalline[J]. *Chem. Eng. J.*, 2017, 330: 1 091-1 099
- [40] Sakurai K, Mizusawa M. X-ray Diffraction Imaging of Anatase and Rutile[J]. *Anal. Chem.*, 2010, 82(9): 3 519-3 522
- [41] Guo Y, Liu Y. Adsorption Properties of Methylene Blue from Aqueous Solution onto Thermal Modified Rectorite[J]. *J. Disper. Sci. Technol.*, 2014, 35(9): 1 351-1 359
- [42] Zhang G, Liu G, Guo Y. Adsorption of Methylene Blue from Aqueous Solution onto Hydrochloric Acid-Modified Rectorite[J]. *J. Wuhan. Univ. Technol.*, 2011, 26(5): 817-822
- [43] Martha S, Reddy KH, Parida KM. Fabrication of In₂O₃ Modified ZnO for Enhancing Stability, Optical Behaviour, Electronic Properties and Photocatalytic Activity for Hydrogen Production under Visible Light[J]. *J. Mater. Chem. A*, 2014, 2(10): 3 621-3 631
- [44] Wu ZW, Li Y G, Gao L J, *et al.* Synthesis of Na-doped ZnO Hollow Spheres with Improved Photocatalytic Activity for Hydrogen Production[J]. *Dalton. Trans.*, 2016, 45(27): 11 145-11 149
- [45] Habibi M H, Hassanzadeh A, Mahdavi S. The Effect of Operational Parameters on the Photocatalytic Degradation of Three Textile Azo Dyes in Aqueous TiO₂ Suspensions[J]. *J. Photochem. Photobiol. A*, 2005, 172(1): 89-96
- [46] Gaya U I, Abdullah A H. Heterogeneous Photocatalytic Degradation of Organic Contaminants over Titanium Dioxide: A Review of Fundamentals, Progress and Problems[J]. *J. Photochem. Photobiol. C*, 2008, 9(1): 1-12
- [47] Fujishima A, Zhang X, Tryk D A. TiO₂ Photocatalysis and Related Surface Phenomena[J]. *Surf. Sci. Rep.*, 2008, 63(12): 515-582
- [48] Oliveira L C A, Gonçalves M, Guerreiro M C, *et al.* A New Catalyst Material Based on Niobia/Iron Oxide Composite on the Oxidation of Organic Contaminants in Water Via Heterogeneous Fenton Mechanisms[J]. *Appl. Catal. A-Gen.*, 2007, 316(1): 117-124
- [49] Shirafuji T, Nomura A, Hayashi Y, *et al.* Matrix-assisted Laser Desorption Ionization Time-of-Flight Mass Spectrometric Analysis of Degradation Products After Treatment of Methylene Blue Aqueous Solution with Three-Dimensionally Integrated Microsolution Plasma[J]. *Jpn. J. Appl. Phys.*, 2016, 55(1s): 01AH02